Phosphoinositide isoforms determine compartment-specific ion channel activity

Xiaoli Zhang, Xinran Li, and Haoxing Xu[1]

Department of Molecular, Cellular, and Developmental Biology, University of Michigan, Ann Arbor, MI 48109

Edited by Richard W. Aldrich, University of Texas at Austin, Austin, TX, and approved May 30, 2012 (received for review February 7, 2012)

Phosphoinositides serve as address labels for recruiting peripheral cytoplasmic proteins to specific subcellular compartments, and as endogenous factors for modulating the activity of integral membrane proteins. Phosphatidylinositol 4,5-bisphosphate ($PI(4,5)P_2$) is a plasma-membrane (PM)–specific phosphoinositide and a positive cofactor required for the activity of most PM channels and transporters. This requirement for phosphoinositide cofactors has been proposed to prevent PM channel/transporter activity during passage through the biosynthetic/secretory and endocytic pathways. To determine whether intracellularly localized channels are similarly "inactivated" at the PM, we studied PIP_2 modulation of intracellular TRPML1 channels. TRPML1 channels are primarily localized in lysosomes, but can also be detected temporarily in the PM upon lysosomal exocytosis. By directly patch-clamping isolated lysosomes, we previously found that lysosomal, but not PM-localized, TRPML1 is active with $PI(3,5)P_2$, a lysosome-specific PIP_2, as the underlying positive cofactor. Here we found that "silent" PM-localized TRPML1 could be activated by depleting $PI(4,5)P_2$ levels and/or by adding $PI(3,5)P_2$ to inside-out membrane patches. Unlike PM channels, surface-expressed TRPML1 underwent a unique and characteristic run-up upon patch excision, and was potently inhibited by a low micromolar concentration of $PI(4,5)P_2$. Conversely, depletion of $PI(4,5)P_2$ by either depolarization-induced activation or chemically induced translocation of 5′-phosphatase potentiated whole-cell TRPML1 currents. $PI(3,5)P_2$ activation and $PI(4,5)P_2$ inhibition of TRPML1 were mediated by distinct basic amino acid residues in a common PIP_2-interacting domain. Thus, $PI(4,5)P_2$ may serve as a negative cofactor for intracellular channels such as TRPML1. Based on these results, we propose that phosphoinositide regulation sets compartment-specific activity codes for membrane channels and transporters.

TRP channel | mucolipin

Although the physiological functions of most ion channels and transporters localized at the cell surface are well established, how channels/transporters localized in intracellular membranes function remains largely unknown. Recent immunohistochemical and electrophysiological studies suggest that the distinctions between the plasma membrane (PM) and intracellular channels/transporters are not strictly defined. Indeed, many PM channels are also found in intracellular compartments (1–3), and intracellular channels such as ER-localized inositol trisphosphate (IP_3) receptors can also be detected at the cell surface (4). These observations raise important questions about whether ion channels/transporters are active in secondary compartments, and whether the same channel protein functions similarly in different subcellular compartments.

Ion channels are intimately regulated by membranous lipids (5), the composition of which differ significantly among distinct membranes (6). Phosphoinositides are compartment-specific phospholipids that play essential roles in various cellular functions, including membrane trafficking and the regulation of membrane potential and neuronal excitability (5, 7, 8). Because phosphoinositides serve as compartment-specific scaffolding recruiters for an array of peripheral cytoplasmic proteins, they are commonly considered to be signature or address labels for specific cellular membranes: phosphatidylinositol 4-phosphate [PI(4)P] for Golgi, phosphatidylinositol 4,5-bisphosphate [$PI(4,5)P_2$] for the PM, phosphatidylinositol 3-phosphate [PI(3)P] for early and late endosomes, and phosphatidylinositol 3,5-bisphosphate [$PI(3,5)P_2$] for late endosomes and lysosomes (LEL) (6). Impaired phosphoinositide signaling leads to aberrant membrane trafficking and mislocalization of proteins and lipids, and hence dysfunctional intracellular organelles (6). Phosphoinositides, especially PIP_2s, also regulate the activity of membrane proteins such as ion channels/transporters (5, 7). Indeed, $PI(4,5)P_2$ appears to serve as a positive cofactor for almost all PM channels/transporters. However, the physiological function of $PI(4,5)P_2$-dependent modulation of PM channels is not clear (9). Because the abundance of $PI(4,5)P_2$ may decrease in response to the activation of Gq/phospholipase C (PLC)–coupled G protein–coupled receptors (GPCRs), it has been proposed that $PI(4,5)P_2$ transduces the information from neurotransmitters into ion channel activity and neuronal excitability (8). Alternatively, a hypothesis put forward by Hilgemann et al. a decade ago proposed that $PI(4,5)P_2$ is the "welcome signal" for PM channels during membrane insertion (7). This model predicts that PM channels are kept inactive or "silent" in compartments without $PI(4,5)P_2$, including the ER and Golgi apparatus within the biosynthetic pathway, and endosomes and lysosomes within the endocytic pathway (1, 2, 9). This hypothesis is attractive because almost all channels/transporters studied thus far are positively regulated by $PI(4,5)P_2$, suggesting that $PI(4,5)P_2$ is a required cofactor for the proper function of PM channels/transporters (10). However, direct evidence to support this hypothesis is still lacking, largely due to the inaccessibility of ion channels in the ER and Golgi apparatus for direct studies (9).

The recent development of endolysosome patch–clamp methods has made studies of ion channels in intracellular organelles, such as endosomes and lysosomes, possible (11, 12). One such channel protein, TRPML1, is primarily a LEL-localized membrane channel protein (13, 14). *TRPML1* mutations cause type IV mucolipidosis (ML4) disease in humans (15) and lysosomal trafficking defects in cells (16). Using whole-endolysosome recordings, we recently found that TRPML1 conducts both Ca^{2+} and Fe^{2+}, and can be activated specifically by $PI(3,5)P_2$ but not other phosphoinositides (12, 16, 17). Interestingly, TRPML1 can also be detected in non-lysosome cellular compartments, in particular, the PM, upon exocytosis from the Golgi apparatus (the biosynthetic pathway) (13, 14) or the lysosome (lysosomal exocytosis) (18, 19). Indeed, when lysosomal exocytosis was dramatically increased by a constitutively active TRPML1 mutant ($TRPML1^{Va}$), large whole-cell TRPML1 currents were detected (18). Because TRPML1 is present at both PM and intracellular membranes, we tested the hypothesis that compartment-specific phosphoinositides determine the compartment-specific activation/inactivation state of TRPML1. In this study, we used whole-cell and inside-out (I/O) patch configurations

Author contributions: X.Z., X.L., and H.X. designed research; X.Z. and X.L. performed research; X.L. contributed new reagents/analytic tools; X.Z. and H.X. analyzed data; and X.Z. and H.X. wrote the paper.

The authors declare no conflict of interest.

This article is a PNAS Direct Submission.

[1]To whom correspondence should be addressed. E-mail: haoxingx@umich.edu.

This article contains supporting information online at www.pnas.org/lookup/suppl/doi:10.1073/pnas.1202194109/-/DCSupplemental.

to study TRPML1 at the PM and whole-endolysosome recordings to study lysosomal TRPML1.

Results

Functional Expression of TRPML1 at the PM. We previously reported that basal whole-endolysosome currents, but not basal whole-cell currents, were observed in HEK293T cells expressing TRPML1-GFP (17, 20). However, in this study using giant (pipette resistance <2 MΩ) inside-out (I/O) cell-free excised patches from TRPML1-GFP–expressing HEK293T cells, we observed single channel openings (in 19 of 29 patches) that were not observed in nontransfected cells (n = 8 patches; Fig. 1*A*). These single-channel currents were inwardly rectifying with a chord conductance of 45 ± 2 pS (from –140 to –40 mV, n = 6; Fig. 1*B* and Fig. S1), which largely resembled the properties of single-channel currents observed in cells expressing TRPML1^{Va}, a gain-of-function, constitutively active TRPML1 mutant (20). Consistent with previous studies on lysosomal TRPML1 (17), PM-localized TRPML1 channels in the I/O patches were robustly activated by bath (cytoplasmic side) application of PI(3,5)P_2 (water-soluble di-C8) in a dose-dependent manner (Fig. S1). Bath application of the TRPML-specific synthetic agonist SF-51 (21) also activated single-channel TRPML1 currents (i_{ML1}) and dramatically enhanced PI(3,5)P_2-induced i_{ML1} (Fig. 1*A*). These results indicate that single-channel TRPML1 currents were detected in the giant I/O patches from TRPML1-overexpressing HEK293T cells, and that PM-localized TRPML1 channels behave similarly to lysosome-localized TRPML1 channels.

TRPML1 Currents Undergo Run-Up in Cell-Free I/O Excised Patches. Upon membrane patch excision, most PM channels undergo rapid channel run-down in I/O membrane patches (5). Strikingly, membrane patch excision into a Mg-ATP-free bath (internal) solution led to the gradual run-up of i_{ML1} over time at the holding potential (HP) of –120 mV (Fig. 1*C*). In contrast, no i_{ML1} openings (NP_o < 0.001; N, channel number; P_o, open probability) were detected in the cell-attached recordings (Fig. 1*C*). The run-up of TRPML1 usually began 30 s after membrane patch excision, and reached a plateau of activity (NP_o = 0.35 ± 0.15, n = 5) within 3–5 min. After reaching a post–run-up steady-state, i_{ML1} could be increased further by PI(3,5)P_2 (100–1,000 nM; Fig. 1*E* and Fig. S1), suggesting that low, but significant basal activity of TRPML1 was detectable at the PM of TRPML1-overepressing cells.

The expression level of wild-type (WT) TRPML1 at the PM is low; thus, for further studies, we used a surface-expressed mutant of TRPML1, in which the lysosome-targeting di-leucine (LL) motifs in both the cytoplasmic N- and C-termini were mutated to alanines (TRPML1-L^{15}L/AA-L^{577}L/AA, abbreviated as ML1–4A) (13, 14, 21). Macroscopic currents were observed in the I/O

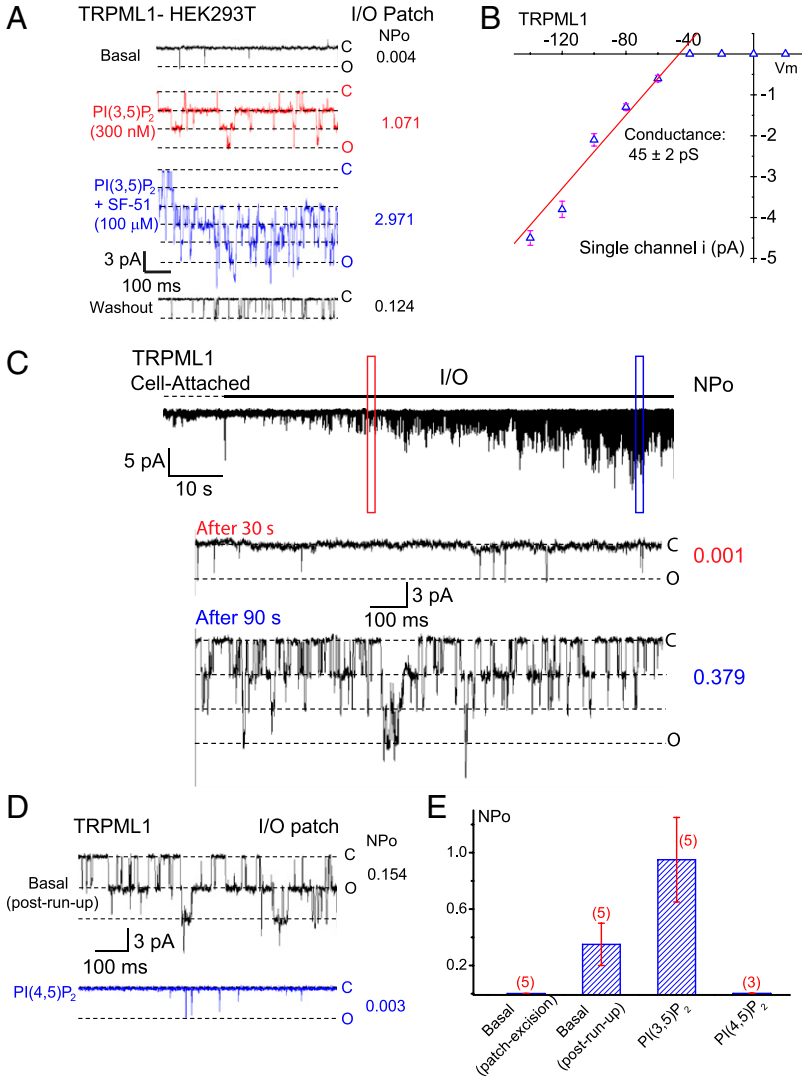

Fig. 1. PI(3,5)P_2 activates and PI(4,5)P_2 inhibits the activity of the PM-localized TRPML1 channel. I/O giant macropatches were excised from the PM of TRPML1-transfected HEK293T cells. The pipette solution contained low pH (4.6) external (modified Tyrode's) solution, and the bath solution was a K^+-based internal/cytoplasmic solution (140 mM K-gluconate; 0 mM ATP). Single channel currents were recorded in the excised patch membranes (HP = –120 mV). C, channel closed state; O, channel open state. (*A*) Representative trace shows sporadic single-channel openings of TRPML1 (basal NP_O = 0.004). Bath application of 300 nM diC8-PI(3,5)P_2 to an I/O patch increased NP_O to 1.071; coapplication of PI(3,5)P_2 and 100 μM SF-51 further enhanced the channel activity (NP_O = 2.971); the stimulatory effects were reversible upon washout of the agonists. (*B*) Single-channel chord conductance of TRPML1 was 45 ± 2 pS (from –140 to –40 mV; n = 6). Single channel TRPML1 currents (i_{ML1}) were activated by PI(3,5)P_2 in I/O patches at different voltages. (*C*) i_{ML1} gradually ran up (NP_O = 0.001 at 30 s, and 0.379 at 90 s after excision) upon membrane patch excision into the bath solution (0 mM ATP). No significant i_{ML1} openings were detected under the cell-attached configuration. Dashed line indicates the cell-attached configuration; solid line indicates the excised I/O patch configuration. (*D*) Post–run-up steady-state i_{ML1} was strongly inhibited by 1 μM PI(4,5)P_2 (NP_O from 0.154 to 0.003). (*E*) Opposite effects of PI(3,5)P_2 and PI(4,5)P_2 on post–run-up i_{ML1}. Data are presented as mean ± SEM; numbers (n) are noted in parentheses.

patches from ML1–4A–expressing HEK293T cells (Fig. 2 *A* and *B*). Consistent with the effects on WT TRPML1 currents, robust run-up of $I_{ML1\text{-}4A}$ was also detected in the excised patches (Fig. 2 *A* and *B*). The run-up of TRPML1 currents in excised membranes, but not in intact cells, suggests the existence of inhibitory factors in the cytoplasmic face of the PM.

Inhibition of TRPML1 by PI(4,5)P_2 in I/O Membrane Patches. The channel run-up observed in TRPML1-containing patches are reminiscent of, although opposite to, the run-down commonly detected with PM channels that require PI(4,5)P_2 as a positive cofactor (5). PI(4,5)P_2 degradation by lipid phosphatases occurs in cytoplasm-free I/O patches; therefore, the application of PI(4,5)P_2 or Mg-ATP that is presumed to be required for lipid kinase–mediated synthesis to maintain tonic PI(4,5)P_2 levels can effectively prevent channel run-down (5). Consistent with this interpretation but in an opposite direction, the inclusion of Mg-ATP in the bath (internal) solution was sufficient to prevent the sensitization/run-up of $I_{ML1\text{-}4A}$ (Fig. S2), and bath application of PI(4,5)P_2 (water-soluble di-C8) largely inhibited post–run-up steady-state i_{ML1} (Fig. 1 *D* and *E*). Likewise, bath application of PI(4,5)P_2 also inhibited post–run-up $I_{ML1\text{-}4A}$ (elicited by a voltage ramp from –140 to +140 mV; Fig. 2 *A* and *B*). In contrast, bath application of PI(3,5)P_2 readily activated i_{ML1} (Fig. 1 *E*) and $I_{ML1\text{-}4A}$ (Fig. 2 *A* and *B*), regardless of whether the I/O patches had been previously exposed to PI(4,5)P_2.

In the I/O patches from HEK293 cells stably expressing ML1–4A, large inward $I_{ML1\text{-}4A}$ was evoked with either 100 nM PI(3,5)P_2 (Fig. 2*C*) or 10 μM SF-51 (Fig. 2*D*). In the presence of the agonists, bath application of PI(4,5)P_2 suppressed the agonist-induced TRPML1 currents in a dose-dependent manner, with an IC_{50} of 0.20 μM for PI(3,5)P_2 (n = 10) and 0.18 μM for SF-51 (n = 5) (Fig. 2 *C–E*), indicative of high affinity compared with most PM channels (5). Because PI(3,5)P_2 and PI(4,5)P_2 are isomers with significant structural similarities, it is possible that PI(4,5)P_2 acted as a competitive antagonist. However, the PI(4,5)P_2-mediated inhibition of both basal (Fig. 1) and SF-51–induced TRPML1 currents suggests that the inhibitory effect was likely direct and independent of PI(3,5)P_2. PI(4,5)P_2 failed to inhibit the gain-of-function $TRPML1^{Va}$ channels (20) (Fig. S3), suggesting a gating effect of PI(4,5)P_2 .

We also investigated the effects of other phosphoinositides on $I_{ML1\text{-}4A}$. PI(3)P, PI(4)P, and PI(5)P (all 300 nM) failed to significantly inhibit PI(3,5)P_2-activated $I_{ML1\text{-}4A}$ (Fig. 2 *F* and *G*), whereas PI(3,4)P_2 and PI(3,4,5)P_3 each caused 60–70% inhibition of PI(3,5)P_2-activated $I_{ML1\text{-}4A}$, comparable to the effect of PI(4,5)P_2 (Fig. 2*G* and Fig. S4). We previously reported that, in a lipid-strip assay, the GST (GST)–fused N terminus of TRPML1 bound to PI(3,5)P_2, PI(4,5)P_2, PI(3,4)P_2, and PI(3,4,5)P_3, but not PI(3)P, PI(4)P, or PI(5)P (17). The correlation between biochemical and electrophysiological results suggests that PI(4,5)P_2 regulates TRPML1 via direct binding. It is worth noting that both PI(3,4)P_2 and PI(3,4,5)P_3 are also generated at the PM, for example, by growth factor signaling or during phagocytosis (6).

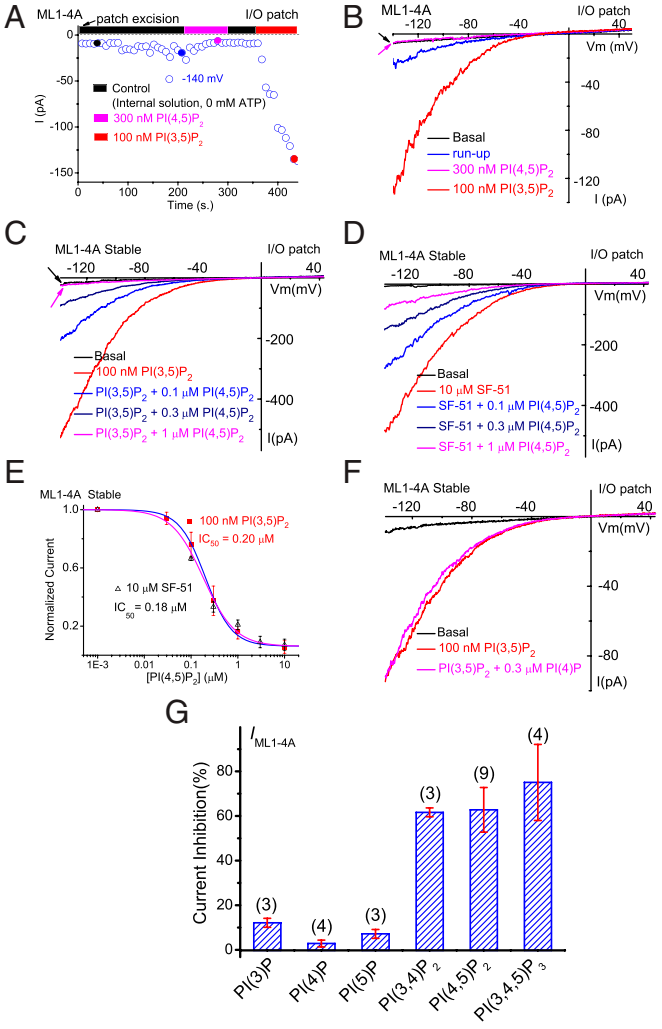

Fig. 2. Agonist-induced TRPML1 channel activity at the PM is suppressed by PI(4,5)P_2. (*A*) $I_{ML1\text{-}4A}$ gradually underwent run-up in an I/O patch, and were inhibited by PI(4,5)P_2 and activated by PI(3,5)P_2. $I_{ML1\text{-}4A}$ were recorded from I/O patches with repeated voltage ramps (from –140 to +140 mV; 400 ms; 4-s interval between ramps). Only a portion of the voltage is shown. Current amplitudes measured at –140 mV were used to plot the time dependence of the PIP_2 effects. The post–run-up $I_{ML1\text{-}4A}$ was strongly inhibited by 300 nM PI(4,5)P_2 but robustly reactivated by 100 nM PI(3,5)P_2. (*B*) Representative traces of $I_{ML1\text{-}4A}$ at the basal level (pre–run-up), post–run-up, and in the presence of PI(4,5)P_2 or PI(3,5)P_2, as indicated by colored circles in *A*. (*C*) Dose-dependent inhibition of PI(3,5)P_2-activated $I_{ML1\text{-}4A}$ by PI(4,5)P_2 in an I/O patch from ML1-4A-expressing HEK293 stable cell lines. (*D*) Dose-dependent inhibition of SF-51–activated $I_{ML1\text{-}4A}$ by PI(4,5)P_2. (*E*) PI(4,5)P_2 inhibited both PI(3,5)P_2-activated and SF-51-activated $I_{ML1\text{-}4A}$ (IC_{50} = 0.2 μM and 0.18 μM, respectively). (*F*) PI(3,5)P_2-activated $I_{ML1\text{-}4A}$ was insensitive to PI(4)P (300 nM). (*G*) Effects of various phosphoinositides on PI(3,5)P_2-activated $I_{ML1\text{-}4A}$. In all experiments, phosphoinositides (300 nM) were coapplied with PI(3,5)P_2 (100 nM). Data are presented as mean ± SEM; numbers (n) are noted in parentheses.

Depletion of PI(4,5)P_2 Potentiates Whole-Cell TRPML1 Currents. If PI(4,5)P_2 inhibits TRPML1, manipulations that decrease the abundance of PI(4,5)P_2 are expected to increase TRPML1 channel activity. We used three different approaches to reduce PI(4,5)P_2 levels in intact cells. First, Gq/PLC-coupled muscarinic M1 receptors were stimulated with the muscarinic agonist carbachol (CCH) in HEK293 cells stably expressing M1 receptors (HM1 cells) (22, 23). The activation of PLC hydrolyzes PI(4,5)P_2 into diacylglycerol (DAG) and IP_3, resulting in significant reduction of PI(4,5)P_2 levels from a basal (resting) concentration of 4–10 μM to 1–3 μM (5, 10, 24). Therefore, the stimulation of PLC-coupled receptors may preferentially regulate ion channels with low, but not high, PI(4,5)P_2 affinity (8). The application of carbachol failed to significantly affect SF-51–activated $I_{ML1\text{-}4A}$ in both ML1–4A-expressing HM1 cells (Fig. S5) and M1 receptor-expressing ML1–4A stable cells. In contrast, carbachol application was sufficient to induce the translocation of the GFP-tagged pleckstrin homology domain of PLCδ1 [GFP-PLCδ1-PH, a PI(4,5)P_2 probe (5)] from plasma membrane to cytosol within seconds (Fig. S5), and readily activated receptor-operated hTRPC6 channels (25) in HM1 cells (Fig. S5). PI(4,5)P_2 reportedly inhibited the OAG-activated TRPC6 current with an IC_{50} of 7.6 μM in the I/O patches (26). Because PI(4,5)P_2 inhibited $I_{ML1\text{-}4A}$ with an IC_{50} of 0.2 μM (Fig. 2*E*), the simplest deduction is that because TRPML1 has a much higher affinity for PI(4,5)P_2 than does TRPC6, the stimulation of

M1 receptors may not be sufficient to release TRPML1 from the tonic inhibition mediated by ambient $PI(4,5)P_2$ levels. Interestingly, the sustained but nonspecific activation of G protein signaling with nonhydrolysable GTP analog, GTP-γ-S (5), evoked small whole-cell $I_{ML1\text{-}4A}$ (Fig. S6).

Depletion of $PI(4,5)P_2$ levels can also be achieved using a rapamycin-dependent heterodimerization system to translocate overexpressed cytosolic 5-phosphatase to the PM, which then irreversibly depletes $PI(4,5)P_2$ levels by converting it into PI(4)P (27). The cytosolic FKBP–5-phosphatase was transfected alone or cotransfected with PM-localized rapamycin-binding protein FRB (PM-FRB) in cells stably expressing ML1–4A. Little or no basal whole-cell $I_{ML1\text{-}4A}$ was detected in ML1–4A stable cells (−20 ± 2 pA at −140 mV, n = 12), or in FKBP–5-phosphatase–transfected cells (Fig. 3 *A* and *B*). Small basal $I_{ML1\text{-}4A}$ was detected in cells cotransfected with PM-FRB and FKBP–5-phosphatase (−113 ± 45 pA, n = 20), but not with PM-FRB and FKBP-5-phosphatase-D281A, a phosphatase-dead mutant (5), suggesting that the "leak" activity of 5-phosphatase might induce small basal $I_{ML1\text{-}4A}$ (Fig. S7). Significantly, rapamycin application evoked large basal $I_{ML1\text{-}4A}$ (−407 ± 81 pA, n = 20; Fig. 3 *A* and *B*).

Furthermore, $PI(4,5)P_2$ depletion can also be achieved in cells transfected with a voltage-sensitive phosphatase from *Ciona intestinalis* (Ci-VSP). Ci-VSP is activated by membrane depolarization ($V_{1/2}$ = +60 mV) (28), converting $PI(4,5)P_2$ into PI(4)P; $PI(4,5)P_2$ levels return in a lipid-kinase–dependent manner upon membrane hyperpolarization (10, 28). In Ci-VSP-transfected ML1–4A stable cells, $I_{ML1\text{-}4A}$ was evoked every 10 s (voltage ramp from −140 to +100 mV; 100 ms) in the presence of 10 μM SF-51. The cells were held at a membrane potential of +80 mV or –60 mV. In Ci-VS– transfected cells, switching the HP from –60 mV to +80 mV gradually increased $I_{ML1\text{-}4A}$ by 4.1- ± 0.4-fold (n = 16). This increase reached a maximum within 8 min, but quickly returned to basal levels upon membrane hyperpolarization to –60 mV (Fig. 3 *C* and *D*). Likewise, depolarization evoked small basal $I_{ML1\text{-}4A}$ (−40.1 ± 6.3 pA at −140 mV, n = 4) in the absence of SF-51 (Fig. S6). No depolarization-induced increase in $I_{ML1\text{-}4A}$ was detected in nontransfected ML1–4A stable cells. The slow activation time course and rapid recovery observed for $I_{ML1\text{-}4A}$ were not observed for other $PI(4,5)P_2$-sensitive channels (10, 23). Hence, we performed a control experiment in Ci-VSP–transfected HEK293T cells and found that, consistent with a previous study (23), TRPM7-like currents (induced by Mg^{2+} removal from both pipette and extracellular solutions) were rapidly suppressed by membrane depolarization and recovered upon membrane hyperpolarization in a relatively slow time course (Fig. 3 *E* and *F*). Therefore, the unique kinetics of the Ci-VSP effect on $I_{ML1\text{-}4A}$ may be explained by the high affinity of TRPML1 for $PI(4,5)P_2$. Collectively, the enhancement of whole-cell $I_{ML1\text{-}4A}$ by the depletion of $PI(4,5)P_2$ levels is consistent with a direct inhibitory effect of $PI(4,5)P_2$ on TRPML1.

Polybasic Domain in Cytoplasmic N Terminus of TRPML1 Is Critical for both $PI(3,5)P_2$ Activation and $PI(4,5)P_2$ Inhibition. Results presented above suggest that $PI(4,5)P_2$ may bind and inhibit TRPML1 directly. Our previous lipid-strip studies showed that $PI(3,5)P_2$, $PI(4,5)P_2$, $PI(3,4)P_2$, and $PI(3,4,5)P_3$, all bind to the GST-fused N terminus of TRPML1 (17). Combined mutations of seven basic amino acid residues (R42Q/R43Q/R44Q/K55Q/R57Q/R61Q/K62Q, abbreviated as 7Q) abolish the binding of all these phosphoinositides, and importantly, prevent $PI(3,5)P_2$ activation of lysosomal TRPML1, suggesting that this lipid-interacting domain (spanning amino acid residues 42–62) is important for the effects of both $PI(3,5)P_2$ and $PI(4,5)P_2$. Although $I_{ML1\text{-}4A\text{-}7Q}$ was not activated by $PI(3,5)P_2$ in I/O patches (Fig. 4 *A* and *B*), SF-51 activation of the channel was relatively intact, suggesting that the activation mechanisms for $PI(3,5)P_2$ and SF-51 are segregated. Unlike $I_{ML1\text{-}4A}$, SF-51–activated $I_{ML1\text{-}4A\text{-}7Q}$ was not significantly inhibited by 1μM $PI(4,5)P_2$ (Fig. 4 *A*–*C*). Consistent with this, $I_{ML1\text{-}4A\text{-}7Q}$ in I/O patches exhibited no obvious run-up. To exclude the possibility that high concentrations of SF-51 (100 μM) may have complex interactions with $PI(4,5)P_2$, $I_{ML1\text{-}4A}$ and $I_{ML1\text{-}4A\text{-}7Q}$

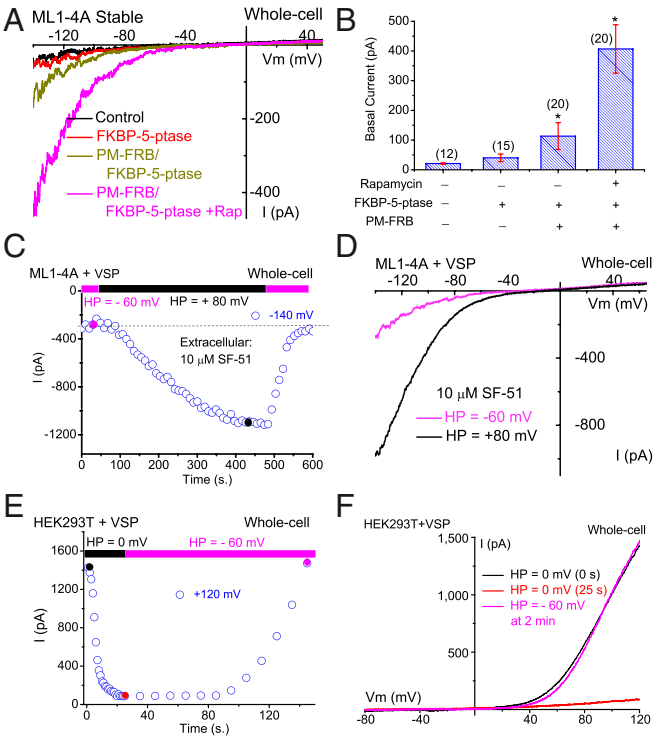

Fig. 3. Depletion of $PI(4,5)P_2$ levels increases whole-cell TRPML1 currents. (*A*) Overexpression of cytosolic FKBP-5′-phosphatase along with rapamycin-induced translocation to the PM enhanced basal whole-cell $I_{ML1\text{-}4A}$. $I_{ML1\text{-}4A}$ was measured in the whole-cell configuration with repeated voltage ramps (from −140 to +140 mV; 400 ms; 4-s interval between ramps; HP = 0 mV). Only a portion of the voltage is shown. The pipette solution contained Cs^+-based internal solution (145 mM Cs-Mes), and the bath was standard external (Tyrode's) solution. HEK293 cells stably expressing ML1–4A were transfected with RFP-FKBP-5-phosphatase alone or together with CFP-PM-FRB, which contains a signal for the PM localization. The dimerization of FRB and FKBP induced by rapamycin (0.5 μM for 10 min) led to translocation of the 5-phosphatase from the cytosol to the PM. (*B*) Summary effects of overexpression and PM translocation of 5-phosphatase on basal $I_{ML1\text{-}4A}$. Rapamycin significantly enhanced basal $I_{ML1\text{-}4A}$. (*C*) Depolarization-activated Ci-VSP 5-phosphatase increased SF-51–activated $I_{ML1\text{-}4A}$ in Ci-VSP–transfected ML1–4A stable cells. $I_{ML1\text{-}4A}$ was elicited by repeated voltage ramps (from −140 mV to +100 mV; 100-ms duration; 10-s interval between ramps; HP = −60 mV or +80 mV). Current amplitudes measured at −140 mV were used to plot the time-dependence of the depolarization-induced effect. (*D*) Representative traces of SF-51-activated $I_{ML1\text{-}4A}$ before (HP = −60 mV, red) and 8 min after (HP = +80 mV, black) Ci-VSP activation at two time points, as shown in *C*. (*E*) Activation of Ci-VSP (HP = 0 mV) led to rapid suppression of endogenous TRPM7-like currents in Ci-VSP–transfected HEK293T cells. TRPM7-like currents were induced by omission of Mg^{2+} in both bath and internal/pipette solutions (HP = -60 mV for >3 min after break-in), and then elicited by repeated voltage ramps (from −100 mV to +120 mV; 100-ms duration; 1- or 10-s interval between ramps; HP = 0 mV or −60 mV). (*F*) Representative I-V traces of TRPM7-like currents before (HP = 0 mV, 0 s) after Ci-VSP activation (HP = 0 mV, 25 s), and after Ci-VSP deactivation (HP = −60 mV, 25 s) at three time points, as shown in *E*. Data are presented as mean ± SEM; numbers (n) are noted in parentheses. Statistical comparisons were performed using analysis of variance. *$P < 0.05$.

were also evoked by the inclusion of SF-51 (100 μM) in the pipette (extracellular) solution whereas $PI(4,5)P_2$ was bath-applied to the intracellular side of the excised membrane (Fig. S8). Under this condition, 1 μM $PI(4,5)P_2$ inhibited $I_{ML1\text{-}4A}$, but not $I_{ML1\text{-}4A\text{-}7Q}$ (Fig. S8). These results suggest that the N-terminal lipid-interacting domain of TRPML1 and the cluster of seven basic residues in the domain are critical not only for $PI(3,5)P_2$ activation but also for $PI(4,5)P_2$ inhibition. Consistent with this, in cells doubly transfected with Ci-VSP and ML1–4A-7Q,

activation of Ci-VSP by depolarization failed to stimulate $I_{ML1\text{-}4A\text{-}7Q}$ (Fig. 4 *D–F*).

Identification of Basic Amino Acid Residues Specific for PI(4,5)P_2 Inhibition, but Not for PI(3,5)P_2 Activation. To further dissect the molecular mechanisms underlying PI(3,5)P_2 activation and PI(4,5)P_2 inhibition, we constructed double- and triple-charge mutants in which charges were removed in the seven basic residues in the ML1–4A background. In analyzing these combined mutations, we found that two of them, R42A/R43A/R44A (abbreviated as 42–44A) and R61A/K62A (abbreviated as 61–62A), exhibited different PIP_2 sensitivities. Although the Ci-VSP–mediated stimulatory effect was largely abolished in whole-cell recordings (Fig. 4*F* and Fig. S8), $I_{ML1\text{-}4A/42\text{–}44A}$ exhibited significantly reduced PI(4,5)P_2 sensitivity in I/O patches (Fig. 4 *G* and *H*). In contrast, $I_{ML1\text{-}4A/42\text{–}44A}$ retained robust PI(3,5)P_2 sensitivity, comparable with that of $I_{ML1\text{-}4A}$ (Fig. 4*I* and Fig. S8). Conversely, the PI(3,5)P_2 sensitivity of $I_{ML1\text{-}4A/61\text{–}62A}$ was substantially diminished (Fig. 4*I*), but its PI(4,5)P_2 sensitivity was only modestly reduced (Fig. 4*H* and Fig. S8). Consistent with these results, in the whole-endolysosome configuration, PI(3,5)P_2 (100 nM) activated large whole-endolysosome $I_{42\text{–}44A}$ (Fig. S8), but not $I_{61\text{–}62A}$. These results suggest that whereas Arg61 and Lys62 were selectively required for PI(3,5)P_2 activation, Arg41/Arg42/Arg43 were specifically required for PI(4,5)P_2 inhibition. Therefore, although this lipid-interacting domain (spanning amino acid residues 42–62) is important for the binding and function of both PI(3,5)P_2 and PI(4,5)P_2, distinct amino acid residues are required for isoform-specific regulation.

Discussion

Unlike PM ion channels, which reside on the intracellular membranes only during vesicular transport through the biosynthetic and/or endocytic pathway, lysosomal channels such as TRPML1 are localized predominantly in the lysosome, but are found temporarily at the cell surface during exocytosis (16). We previously reported that TRPML1 is active in the LEL, but not in the PM, and that a LEL-localized PIP_2, PI(3,5)P_2, is responsible for the activity of TRPML1 in LEL. In this study, we found that TRPML1, localized in the PM due to high levels of overexpression and mutation of the lysosome-targeting motifs, can become active upon the depletion of PI(4,5)P_2 or the addition of PI(3,5)P_2. Indeed, although TRPML1 is directly and potently inhibited by PI(4,5)P_2 in I/O patches, the degradation of PI(4,5)P_2 by overexpression and PM-translocation of 5-phosphatase is sufficient to activate and potentiate whole-cell TRPML1 currents. Interestingly, PI(4,5)P_2 inhibition, but not PI(3,5)P_2 activation, is diminished by mutations of three basic amino acid residues in the TRPML1 N-terminal PIP_2-interacting domain that is critical for both binding (17) and functional effects of PI(4,5)P_2 and PI(3,5)P_2. Thus, inhibition by PI(4,5)P_2 may serve as a mechanism to inactivate lysosome-operating TRPML1 channels upon PM insertion. Given these results, we propose that phosphoinositide regulation establishes compartment-specific activity codes for membrane channels and transporters.

The inhibitory effects of the PM-specific phosphoinositides PI(4,5)P_2, PI(3,4,5)P_3, and PI(3,4)P_2, the stimulatory effect of LEL-specific PI(3,5)P_2, and the lack of effect of Golgi-specific PI(4)P or early endosome-specific PI(3)P, indicate that a tight regulatory mechanism controls TRPML1 activity during membrane trafficking. TRPML1 plays a key role in Ca^{2+}-dependent lysosomal exocytosis, a cellular process that is important for membrane repair and neurotransmitter release (18, 19). Phosphoinositide-mediated activation of TRPML1 may lead to lysosomal Ca^{2+} release, triggering lysosome exocytosis (17, 18). Subsequently, the agonist-bound TRPML1, together with its activation machinery, is inserted into the PM to face a large electrochemical Ca^{2+} gradient (across the PM). Notably, TRPML1 exhibits slow desensitization in response to agonist stimulation and is not inactivated by voltage stimulation (16). However, it is necessary to rapidly turn off Ca^{2+} influx, which otherwise would lead to Ca^{2+} overload and cell death, as shown in cells expressing the gain-of-

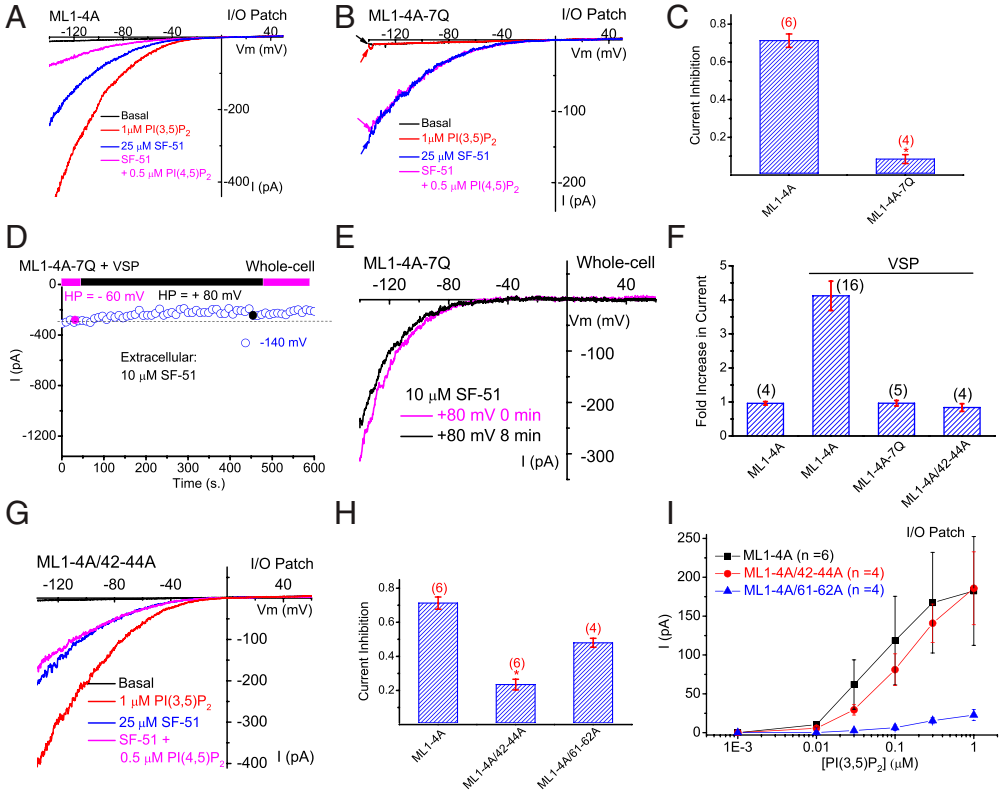

Fig. 4. Structural determinants of PI(4,5)P_2 inhibition of TRPML1. (*A*) In an I/O patch from ML1–4A–expressing HEK293 cells, $I_{ML1\text{-}4A}$ activated by SF-51 (25 μM; bath application) was significantly inhibited by PI(4,5)P_2 (0.5 μM). PI(3,5)P_2 (1 μM) activated $I_{ML1\text{-}4A}$ in the same patch. (*B*) SF-51–activated $I_{ML1\text{-}4A\text{-}7Q}$ was insensitive to PI(4,5)P_2 (0.5 μM), and $I_{ML1\text{-}4A\text{-}7Q}$ was not activated by PI(3,5)P_2 (1 μM) in the same patch. (*C*) Bar graph depicting the insensitivity of ML1-4A-7Q to PI(4,5)P_2. (*D* and *E*) 7Q mutations abolished the effect of Ci-VSP activation (HP = +80 mV, 8 min) of ML1–4A. (*F*) 7Q mutations and triple mutations (R42A/R43A/R44A) abolished the stimulatory effect of Ci-VSP on ML1–4A. (*G*) ML1–4A/42–44A was only slightly inhibited by PI(4,5)P_2, but robustly activated by PI(3,5)P_2. (*H*) Bar graph depicting the sensitivity of ML1–4A/42–44A and ML1–4A/61–62A to PI(4,5)P_2 inhibition (ML1–4A data were replotted from *C* for comparison). (*I*) ML1–4A/42–44A, but not ML1–4A/61–62A, remained sensitive to PI(3,5)P_2 activation. Data are presented as mean ± SEM; numbers (*n*) are noted in parentheses. Statistical comparisons were performed using analysis of variance. *$P < 0.05$.

function mutant TRPMLs (29). Although rapid on-and-off switching of phosphoinositide kinase and phosphatase activity to deplete $PI(3,5)P_2$ may occur after membrane insertion (6, 9), the recruitment of $PI(4,5)P_2$ to the vicinity of the activated TRPML1 may provide an additional potent shut-off mechanism. In this regard, compartment-specific phosphoinositides provide an economical and efficient means to regulate TRPML1 channel activity in a compartment-specific manner.

TRPML1 provides a unique opportunity to study the structural mechanisms and specificities of PIP_2 regulation in ion channels, because two similar isomers of PIP_2 bind to the same PIP_2-interacting domain to exert opposite effects. Within this domain, we have identified amino acid residues that are critical for $PI(3,5)P_2$ activation of TRPML1, such as Arg61 and Lys62, as well as residues that are critical only for the $PI(4,5)P_2$ inhibition. Recent crystallography studies on Kir channels have demonstrated that multiple basic residues widely spaced in sequence in both the *N*- and C-termini fold together to interact with the phosphate groups of $PI(4,5)P_2$, inducing an extensive structural rearrangement to facilitate channel opening (30, 31). Based on our mutational analyses, it is possible that R42/R43/R44 participate in binding to the 4′phosphate in the inositide ring, and R61/K62 participate in binding to the 3′phosphate. The physiological significance of $PI(4,5)P_2$ modulation of TRPML1 can be tested with in vivo models using the 42–44A mutations. Future studies may reveal whether other lysosomal channels also exhibit $PI(3,5)P_2$ dependence and $PI(4,5)P_2$ inhibition, whether channels localized in other compartments are modulated by their compartment-specific signature phospholipids, and whether PM channels are "shut-down" in intracellular compartments. Based on our current studies, we propose that in addition to their roles as physical localization signals for peripheral proteins, compartment-specific phosphoinositides serve as functional localization signals for membrane proteins.

Materials and Methods

Molecular Biology and Biochemistry. Full-length mouse TRPML1 cDNA was cloned into the EGFP-C2 vector (Clontech) as described previously (20). The surface-expressing mutant of TRPML1, TRPML1-L_{15}L/AA-L_{577}L/AA (ML1–4A), was constructed using a site-directed mutagenesis kit (Qiagen). All constructs were confirmed by sequencing.

TRPML1–4A Stable Cell Lines. HEK293 cells stably expressing ML1–4A were created using the FLP-in Tet-On system (Invitrogen), and were maintained in DMEM-F12 medium with 10% (vol/vol) Tet-free FBS and 0.5 μg/mL hygromycin. To induce expression of ML1–4A, doxycycline (1 μg/mL) was added to the culture medium, and cells were incubated overnight.

Whole-Cell Electrophysiology. Whole-cell recordings were obtained from transfected cells using pipette electrodes (resistance 3–5 MΩ) filled with the following (in mM): 147 Cs, 120 methane-sulfonate, 4 NaCl, 10 EGTA, 2 Na_2-ATP, 2 $MgCl_2$, and 20 Hepes (pH 7.2; free $[Ca^{2+}]_i$ < 10 nM), or 140 K-gluconate, 4 NaCl, 1 EGTA, 2 $MgCl_2$, 0.39 $CaCl_2$, and 20 Hepes (pH 7.2; free $[Ca^{2+}]_i$ ~100 nM). The standard extracellular bath solution (modified Tyrode's solution) contained (in mM): 153 NaCl, 5 KCl, 2 $CaCl_2$, 1 $MgCl_2$, 20 Hepes, and 10 glucose (pH 7.4). All bath solutions were applied via a perfusion system to achieve a complete solution exchange within a few seconds. Data were collected using an Axopatch 2A patch clamp amplifier, Digidata 1440, and pClamp 10.0 software (Axon Instruments). Whole-cell currents were digitized at 10 kHz and filtered at 2 kHz. All experiments were conducted at room temperature (21–23 °C), and all recordings were analyzed with pClamp 10.0 and Origin 8.0 (OriginLab).

I/O Electrophysiology. For giant excised-patch recordings, polished pipette electrodes (resistance 1–2 MΩ) were filled with a low pH Tyrode's solution containing the following (in mM): 150 Na-Gluconate, 5 KCl, 2 $CaCl_2$, 1 $MgCl_2$, 10 glucose, 10 Hepes, and 10 Mes (pH 4.6). Unless otherwise stated, bath (internal/cytoplasmic) solution contained (in mM): 140 K-gluconate, 4 NaCl, 1 EGTA, 2 $MgCl_2$, 0.39 $CaCl_2$, and 20 Hepes (pH 7.2; free $[Ca^{2+}]_i$ ~100 nM). In a subset of experiments, 2 mM Na_2-ATP was added to the bath solution, and the pH was readjusted.

Endolysosomal Electrophysiology. Whole endolysosome recordings were performed in isolated enlarged LELs from Cos-1 cells transfected with TRPML1 or its mutants, as described previously (12, 17). Briefly, the transfected cells were treated with 1 μM vacuolin-1 for 2–5 h to increase the size of LELs (up to 5 μm). Vacuoles were released from a cell by peeling off the cell membrane with a thin pipette electrode. Bath (internal/cytoplasmic) solution contained (in mM): 140 K-Gluconate, 4 NaCl, 1 EGTA, 2 Na_2-ATP, 2 $MgCl_2$, 0.39 $CaCl_2$, and 10 Hepes (pH 7.2; free $[Ca^{2+}]_i$ ~100 nM). Pipette (luminal) solution was a low pH "Tyrode" solution that contained (in mM): 145 NaCl, 5 KCl, 2 $CaCl_2$, 1 $MgCl_2$, 10 Mes, 10 Hepes, and 10 glucose (pH 4.6).

ACKNOWLEDGMENTS. The authors thank Dr. Yasushi Okamura for the Ci-VSP plasmid and Dr. Tamas Balla for the CFP-PM-FRB and RFP-FKBP-5-ptase constructs. This work was supported by National Institutes of Health Grant R01-NS062792 (to H.X.) and a postdoctoral fellowship grant from the ML4 Foundation (to X.Z.).

1. Krapivinsky G, Mochida S, Krapivinsky L, Cibulsky SM, Clapham DE (2006) The TRPM7 ion channel functions in cholinergic synaptic vesicles and affects transmitter release. *Neuron* 52:485–496.
2. Montell C (2006) An exciting release on TRPM7. *Neuron* 52:395–397.
3. Dong XP, Wang X, Xu H (2010) TRP channels of intracellular membranes. *J Neurochem* 113:313–328.
4. Dellis O, et al. (2006) Ca2+ entry through plasma membrane IP3 receptors. *Science* 313:229–233.
5. Suh BC, Hille B (2008) PIP2 is a necessary cofactor for ion channel function: How and why? *Annu Rev Biophys* 37:175–195.
6. Di Paolo G, De Camilli P (2006) Phosphoinositides in cell regulation and membrane dynamics. *Nature* 443:651–657.
7. Hilgemann DW, Feng S, Nasuhoglu C (2001) The complex and intriguing lives of PIP2 with ion channels and transporters. *Sci STKE* 2001:re19.
8. Gamper N, Shapiro MS (2007) Regulation of ion transport proteins by membrane phosphoinositides. *Nat Rev Neurosci* 8:921–934.
9. Falkenburger BH, Jensen JB, Dickson EJ, Suh BC, Hille B (2010) Phosphoinositides: Lipid regulators of membrane proteins. *J Physiol* 588:3179–3185.
10. Suh BC, Leal K, Hille B (2010) Modulation of high-voltage activated Ca(2+) channels by membrane phosphatidylinositol 4,5-bisphosphate. *Neuron* 67:224–238.
11. Saito M, Hanson PI, Schlesinger P (2007) Luminal chloride-dependent activation of endosome calcium channels: Patch clamp study of enlarged endosomes. *J Biol Chem* 282:27327–27333.
12. Dong XP, et al. (2008) The type IV mucolipidosis-associated protein TRPML1 is an endolysosomal iron release channel. *Nature* 455:992–996.
13. Pryor PR, Reimann F, Gribble FM, Luzio JP (2006) Mucolipin-1 is a lysosomal membrane protein required for intracellular lactosylceramide traffic. *Traffic* 7:1388–1398.
14. Vergarajauregui S, Puertollano R (2006) Two di-leucine motifs regulate trafficking of mucolipin-1 to lysosomes. *Traffic* 7:337–353.
15. Sun M, et al. (2000) Mucolipidosis type IV is caused by mutations in a gene encoding a novel transient receptor potential channel. *Hum Mol Genet* 9:2471–2478.
16. Cheng X, Shen D, Samie M, Xu H (2010) Mucolipins: Intracellular TRPML1-3 channels. *FEBS Lett* 584:2013–2021.
17. Dong XP, et al. (2010) PI(3,5)P(2) Controls Membrane Traffic by Direct Activation of Mucolipin Ca Release Channels in the Endolysosome. (Translated from English) *Nat Commun* 1:38.
18. Dong XP, et al. (2009) Activating mutations of the TRPML1 channel revealed by proline-scanning mutagenesis. *J Biol Chem* 284:32040–32052.
19. Medina DL, et al. (2011) Transcriptional activation of lysosomal exocytosis promotes cellular clearance. *Dev Cell* 21:421–430.
20. Xu H, Delling M, Li L, Dong X, Clapham DE (2007) Activating mutation in a mucolipin transient receptor potential channel leads to melanocyte loss in varitint-waddler mice. *Proc Natl Acad Sci USA* 104:18321–18326.
21. Grimm C, et al. (2010) Small molecule activators of TRPML3. *Chem Biol* 17:135–148.
22. Xu H, Delling M, Jun JC, Clapham DE (2006) Oregano, thyme and clove-derived flavors and skin sensitizers activate specific TRP channels. *Nat Neurosci* 9:628–635.
23. Xie J, et al. (2011) Phosphatidylinositol 4,5-bisphosphate (PIP(2)) controls magnesium gatekeeper TRPM6 activity. *Sci Rep* 1:146.
24. Xu C, Watras J, Loew LM (2003) Kinetic analysis of receptor-activated phosphoinositide turnover. *J Cell Biol* 161:779–791.
25. Wu LJ, Sweet TB, Clapham DE (2010) International Union of Basic and Clinical Pharmacology. LXXVI. Current progress in the mammalian TRP ion channel family. *Pharmacol Rev* 62:381–404.
26. Albert AP, Saleh SN, Large WA (2008) Inhibition of native TRPC6 channel activity by phosphatidylinositol 4,5-bisphosphate in mesenteric artery myocytes. *J Physiol* 586: 3087–3095.
27. Suh BC, Inoue T, Meyer T, Hille B (2006) Rapid chemically induced changes of PtdIns (4,5)P2 gate KCNQ ion channels. *Science* 314:1454–1457.
28. Murata Y, Iwasaki H, Sasaki M, Inaba K, Okamura Y (2005) Phosphoinositide phosphatase activity coupled to an intrinsic voltage sensor. *Nature* 435:1239–1243.
29. Grimm C, Jörs S, Heller S (2009) Life and death of sensory hair cells expressing constitutively active TRPML3. *J Biol Chem* 284:13823–13831.
30. Hansen SB, Tao X, MacKinnon R (2011) Structural basis of PIP2 activation of the classical inward rectifier K+ channel Kir2.2. *Nature* 477:495–498.
31. Whorton MR, MacKinnon R (2011) Crystal structure of the mammalian GIRK2 K+ channel and gating regulation by G proteins, PIP2, and sodium. *Cell* 147:199–208.

Supporting Information

Zhang et al. 10.1073/pnas.1202194109

SI Discussion

Although carbachol activated the M1 receptor/Gq/PLC pathway, leading to the hydrolysis of $PI(4,5)P_2$ and activation of TRPC6, it failed to stimulate TRPML1 activity. In contrast, the breakdown of $PI(4,5)P_2$ by direct activation of 5-phosphatase was sufficient to activate TRPML1. One potential explanation for this discrepancy is that the affinity of ion channels determines their sensitivity to $PI(4,5)P_2$ (1). The insensitivity of TRPML1 to M1 receptor activation might reflect the channel's high affinity to $PI(4,5)P_2$ (IC_{50} = 0.2 μM). Although we observed a rapid carbachol-induced translocation of GFP-PLCδ1-PH, a commonly used $PI(4,5)P_2$ probe with a K_d of 1.7 μM (2), it remains unknown whether M1 receptor activation could sufficiently deplete the $PI(4,5)P_2$ level to modulate TRPML1. Moreover, activation of TRPML1 by GTP-γ-S, but not M1 receptor activation, could potentially be explained by a "receptor-specific phosphoinositide signaling" theory that highlights the importance of a local $PI(4,5)P_2$ pool in regulating the channels only adjacent to the receptors (3). Finally, the insensitivity of TRPML1 to M1 receptor/PLC activation could also be explained by the fact that receptor stimulation might activate other signaling pathways such as diacylglycerol, inositol triphosphate, Ca^{2+}, and PKC, concurrently to nullify the effect of $PI(4,5)P_2$ depletion on TRPML1 activation.

1. Suh BC, Hille B (2008) PIP2 is a necessary cofactor for ion channel function: How and why? *Annu Rev Biophys* 37:175–195.
2. Lemmon MA, Ferguson KM, O'Brien R, Sigler PB, Schlessinger J (1995) Specific and high-affinity binding of inositol phosphates to an isolated pleckstrin homology domain. *Proc Natl Acad Sci USA* 92:10472–10476.
3. Gamper N, Shapiro MS (2007) Regulation of ion transport proteins by membrane phosphoinositides. *Nat Rev Neurosci* 8:921–934.

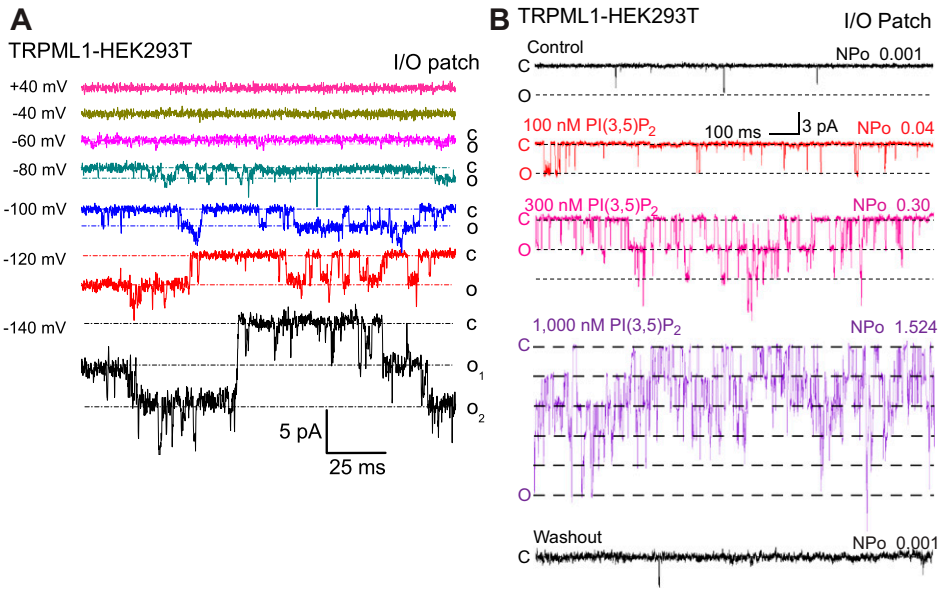

Fig. S1. Single-channel currents in an I/O patch excised from a TRPML1-expressing HEK293T cell. (*A*) Single-channel openings were elicited using a voltage step protocol from −140 mV to +80 mV (HP = 0 mV). At negative, but not positive potentials, channel openings were frequently observed. C, closed state; O, open state. (*B*) $PI(3,5)P_2$ activates single channel TRPML1 currents at the plasma membrane (PM) in a dose-dependent manner. The $PI(3,5)P_2$ effect was examined in an I/O patch excised from TRPML1-GFP–expressing HEK293T cells.

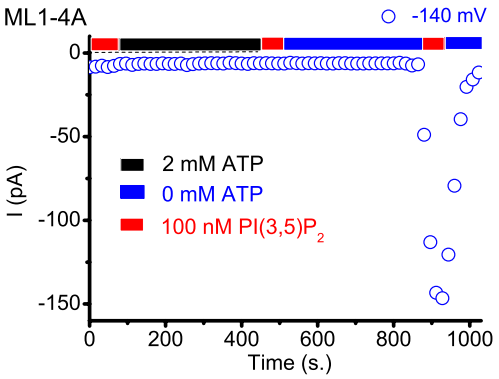

Fig. S2. Mg-ATP prevents run-up of TRPML1 currents in I/O patches. In an I/O patch, bath application of 2 mM Mg-ATP for 6 min prevented run-up of ML1-4A. Upon removal of Mg-ATP for 6 min, $I_{ML1\text{-}4A}$ was activated by 100 nM PI(3,5)P_2.

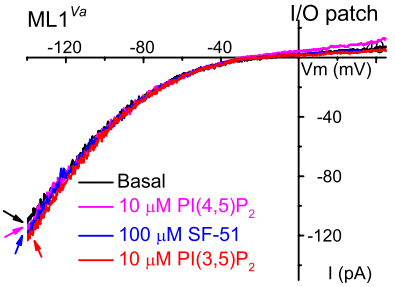

Fig. S3. Insensitivity of TRPML1^{Va} to PI(4,5)P_2. Large basal $I_{ML1\text{-}Va}$ was detected in an I/O patch excised from ML1^{Va}-expressing cells. PI(4,5)P_2 (10 μM) failed to inhibit $I_{ML1\text{-}Va}$.

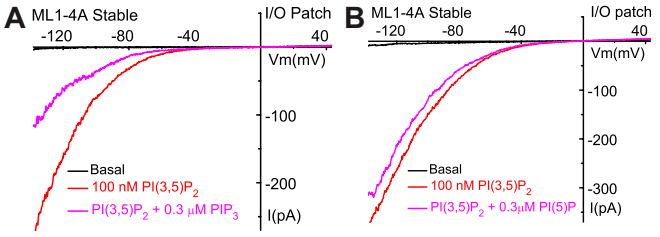

Fig. S4. Effects of PI(3,4,5)P_3 and PI(5)P on $I_{ML1\text{-}4A}$. (*A*) Inhibition PI(3,5)P_2-activated $I_{ML1\text{-}4A}$ by 300 nM PI(3,4,5)P_3 in an I/O patch excised from ML1-4A stable cells. (*B*) Lack of an effect of PI(5)P (300 nM) on PI(3,5)P_2-activated $I_{ML1\text{-}4A}$.

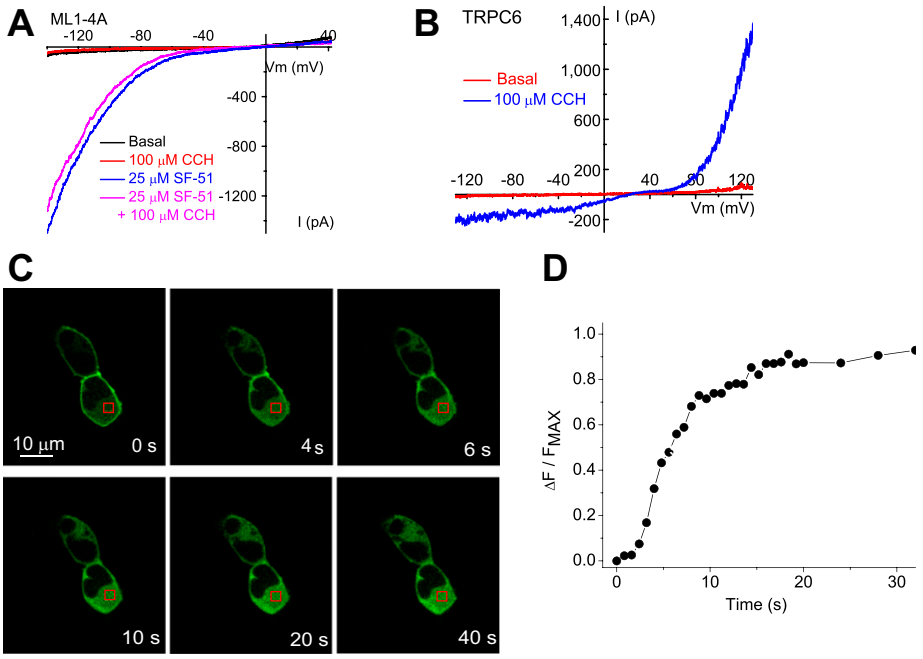

Fig. S5. Receptor-mediated activation of PLC induces PI(4,5)P_2 hydrolysis but fails to activate TRPML1. (*A*) Activation of PLC-coupled M1 receptors had no effect on $I_{ML1\text{-}4A}$. Carbachol (CCH; 100 μM) was used to activate the Gq/PLC pathway in HM1 cells. (*B*) Whole-cell TRPC6 currents were activated by CCH (100 μM). (*C* and *D*) CCH-induced hydrolysis of PI(4,5)P_2 detected using a PI(4,5)P_2 probe. (C) CCH (100 μM) induced a translocation of GFP–PLCδ1-PH from the plasma membrane to the cytosol. Images shown were taken 0, 4, 6, 10, 20, and 40 s after CCH application. Red boxes indicate cytosolic regions where fluorescence intensity (F) was measured. (*D*) Time course of GFP–PLCδ1-PH translocation. Changes in average fluorescence intensity ($\Delta F = F - F_{basal}$) are normalized to maximum change of fluorescence intensity (F_{max}) and plotted with time. Data were analyzed with ImageJ software (National Institutes of Health).

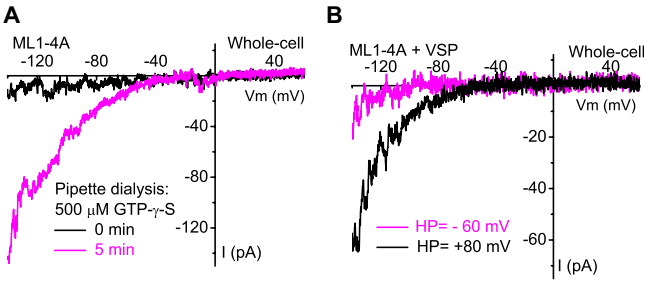

Fig. S6. GTP-γ-S and depolarization-activated Ci-VSP evoke whole-cell TRPML1 currents. (*A*) In an HM1 cell overexpressing TRPML1-4A, small whole-cell $I_{ML1\text{-}4A}$ developed gradually upon pipette dialysis of GTP-γ-S (500 μM) for 5 min. (*B*) Depolarization-activated Ci-VSP increases basal $I_{ML1\text{-}4A}$. Representative traces of whole-cell currents in Ci-VSP–transfected ML1–4A stable cells before (HP = –60 mV) and 8 min after depolarization (HP = +80 mV). $I_{ML1\text{-}4A}$ was elicited by voltage ramps (from –140 mV to +100 mV; 100-ms duration).

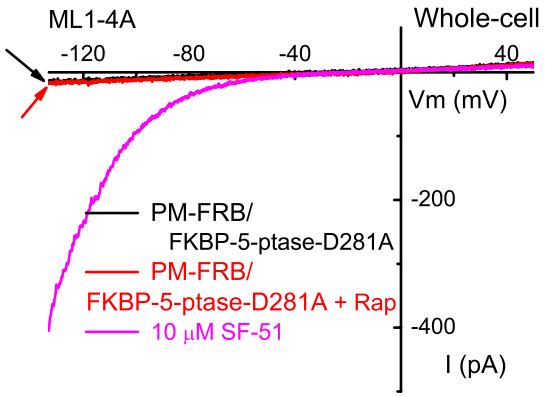

Fig. S7. PM-translocation of inactive mutant FKBP-5-phosphatase fails to activate whole-cell TRPML1 currents. No detectable $I_{ML1\text{-}4A}$ was observed with or without Rapamycin (0.5 μM) application in ML1–4A –expressing HEK293 stable cells transfected with inactive mutant (D281A) of FKBP-5-phosphatase (FKBP-5-ptase-D281A) together with PM-FRB, which contains a signal for the PM localization. The dimerization of FRB and FKBP induced by rapamycin (0.5 μM for 10 min) led to translocation of 5-phosphatase from the cytosol to the PM. $I_{ML1\text{-}4A}$ was readily activated by SF-51 in the same cell.

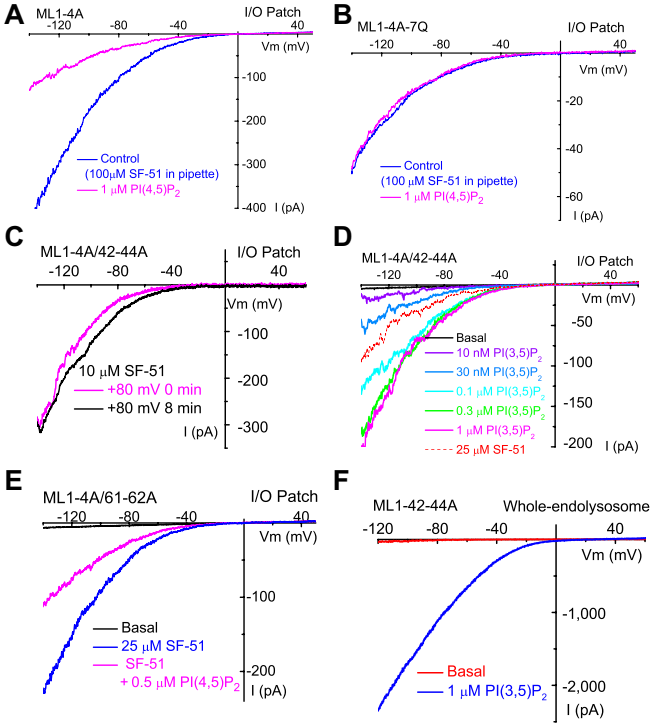

Fig. S8. Mutational analysis of $PI(4,5)P_2$ inhibition and $PI(3,5)P_2$ activation of TRPML1. (*A* and *B*) $PI(4,5)P_2$ inhibition is abolished by 7Q mutations in I/O patches. (*A*) Activation of $I_{ML1\text{-}4A}$ by SF-51 (100 μM; included in pipette solution) was significantly inhibited by bath application of $PI(4,5)P_2$ (1 μM). (*B*) Activation of $I_{ML1\text{-}4A\text{-}7Q}$ by SF-51 (100 μM; included in pipette solution) was insensitive to $PI(4,5)P_2$ (1 μM). (*C*) Triple mutations in the PIP_2-interacting domain abolish the activation effect of Ci-VSP. Activation of Ci-VSP by depolarization (HP = +80 mV) failed to potentiate the SF-51(10 μM)-activated $I_{ML1\text{-}4A/42\text{–}44A}$. (*D*) Dose-dependent activation of ML1–4A/42–44A by $PI(3,5)P_2$. $I_{ML1\text{-}4A/42\text{–}44A}$ was activated by various concentrations of $PI(3,5)P_2$ (10 nM, 30 nM, 0.1 μM, 0.3 μM, and 1 μM). Effect of SF-51 (25 μM) is shown for comparison. (*E*) $PI(4,5)P_2$ sensitivity of R61A/K62A double mutations. Activation of $I_{ML1\text{-}4A/61\text{–}62A}$ by SF-51 (25 μM) was inhibited by $PI(4,5)P_2$ (0.5 μM). (*F*) Activation of ML1-42–44A by $PI(3,5)P_2$ in the lysosome. Whole-endolysosome $I_{42\text{–}44A}$ was robustly activated by $PI(3,5)P_2$ (1 μM).